

Long-Term Fluorescent Cellular Tracing by the Aggregates of AIE Bioconjugates

Zhengke Wang,^{†,‡,⊥,§} Sijie Chen,^{†,⊥,§} Jacky W. Y. Lam,^{†,⊥} Wei Qin,[†] Ryan T. K. Kwok,[†] Ni Xie,[†] Qiaoling Hu,[‡] and Ben Zhong Tang^{*,†,||,⊥}

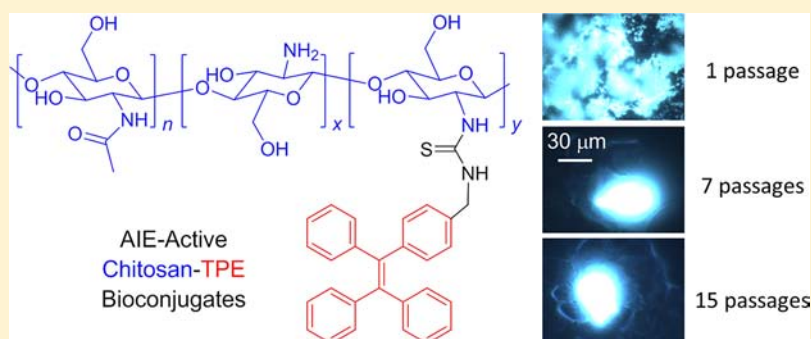
[†]Department of Chemistry, Division of Biomedical Engineering, Institute for Advanced Study, and Institute of Molecular Functional Materials, The Hong Kong University of Science and Technology (HKUST), Clear Water Bay, Kowloon, Hong Kong, China

[‡]Institute of Biomedical Macromolecules, MoE Key Laboratory of Macromolecular Synthesis and Functionalization, Zhejiang University, Hangzhou 310027, China

^{||}Guangdong Innovative Research Team, SCUT-HKUST Joint Research Laboratory, State Key Laboratory of Luminescent Materials and Devices, South China University of Technology (SCUT), Guangzhou 510640, China

[⊥]HKUST Shenzhen Research Institute, Nanshan, Shenzhen 518057, China

Supporting Information



ABSTRACT: There is a great demand for long-term cellular tracers because of their great importance in monitoring biological processes, pathological pathways, therapeutic effects, etc. Herein we report a new type of fluorescence “turn-on” probe for tracing live cells over a long period of time. We synthesized the fluorogenic probe by attaching a large number of tetraphenylethene (TPE) labels to a chitosan (CS) chain. The resultant TPE–CS bioconjugate shows a unique aggregation-induced emission (AIE) behavior. It is nonfluorescent when dissolved but becomes highly emissive when its molecules are aggregated. The AIE aggregates can be readily internalized by HeLa cells. The cellular staining by the TPE–CS aggregates is so indelible that it enables cell tracing for as long as 15 passages. The internalized AIE aggregates are kept inside the cellular compartments and do not contaminate other cell lines in the coculture systems, permitting the differentiation of specific cancerous cells from normal healthy cells.

1. INTRODUCTION

The development of long-lasting cellular tracers is of great scientific value and has important practical implications, for such tracers may enable biological researchers and medicinal practitioners to systematically and continuously follow cell transplantation, migration, division, fusion, and lysis to study cancer pathogenesis, invasion, and metastasis, to monitor flow and circulation in capillaries, to examine neural network and neuronal connectivity, to scrutinize cellular movements in tissues and organisms, etc. over a large time span on site and in time.¹

Fluorescent molecules have been widely used as biological imaging reagents.^{2,3} When the fluorophores are added into culture media of live cells, the small molecules can penetrate into cellular interiors, often due to the concentration gradient in the extra- and intracellular fluorophores. However, when the

confluent cells are passaged, the internalized dyes can be extruded out to the fresh growth media, due to the reverse gradient in the fluorophore concentrations. Because of the poor intracellular retention of the molecular species, most of the conventional fluorophores are unsuitable for long-term cellular tracing applications.²

Various approaches have been taken in order to keep the dyes inside cells.² A number of chemical reactions have been utilized to fix fluorophoric units to the cellular components, typical examples of which include thiol- and amine-mediated reactions,² with the azide–alkyne click reaction being the new development in the area of research.^{4,5} However, the in situ covalent attachment of the synthetic dyes to the intracellular

Received: December 27, 2012

Published: May 13, 2013

biopolymers may alter their chain conformations and folding patterns and thus exert undesired effects on the physiological functions and metabolic processes of the cellular components. The use of the Cu-based catalysts in the click reactions is an issue of serious concern, owing to the severe cytotoxicity of the metallic species.

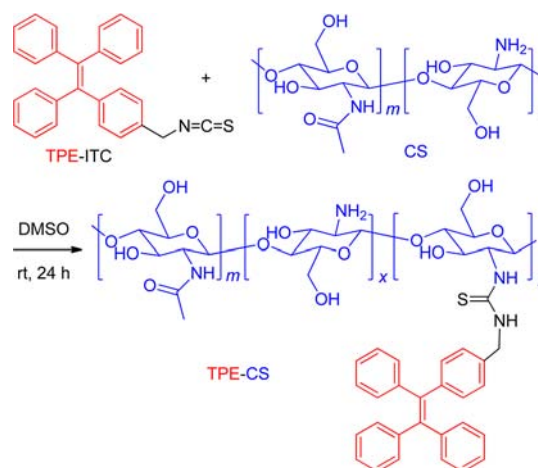
Another approach taken by the researchers in the area is to label biomacromolecules (e.g., proteins and dextrans) with fluorophores through bioconjugation reactions outside cells under abiotic conditions.² Although this approach can avoid the problems associated with the intracellular reactions, it has other drawbacks. For example, the protein bioconjugates may be readily decomposed by enzymatic proteolysis. The dextran bioconjugates, on the other hand, are membrane-impermeant and usually need to be loaded onto cells by harsh and invasive techniques or processes, such as microinjection, electroporation, whole-cell patch clamping, perfusion, scrape loading, microprojectile bombardment, and hypotonic shock, which may harm cellular health and cause cellular infection or even lysis.²

Fluorescence output of a bioconjugate is often limited by the degree of labeling (DL) or number of fluorescent labels that are attached to a biopolymer chain. A high DL frequently does not lead to an enhanced but to a weakened emission, due to the notorious aggregation-caused quenching (ACQ) effect on the fluorescence process.⁶ In a heavily labeled bioconjugate, the aromatic fluorophores tend to aggregate in aqueous media, generating such detrimental species as excimers. The excimer formation prompts nonradiative decays of the excited states and quenches fluorescence of the bioconjugate. For example, fluorescence of heavily labeled casein conjugates is quenched to a level of typically <3% of that of their corresponding free fluorophores.² Although more fluorophores can be loaded onto microspheres of synthetic polymers (e.g., polystyrene beads) through elaborate control, the ACQ problem still persists, hampering the fabrication of highly emissive polymer beads.²

We have observed a unique photophysical process termed aggregation-induced emission (AIE),^{7–10} which is opposite to the common ACQ effect discussed above.⁶ An AIE fluorogen is virtually nonemissive as an isolated molecule but becomes highly fluorescent in the aggregate state.^{7–13} Tetraphenylsilole (TPS)⁹ and tetraphenylethene (TPE)¹⁰ are two archetypical AIE fluorogens. In our previous work, we synthesized a TPS derivative.¹⁴ Whereas conventional dyes (e.g., MitoTracker Green FM) could stain HeLa cells for only one passage, the aggregates of the TPS derivative could trace the cells for four passages.¹⁴ In another work, we fabricated nanoparticles of a TPE-decorated fumaronitrile using lipid–poly(ethylene glycol) complexes as the coencapsulation matrixes. The nanoparticle surfaces were further functionalized by an HIV-1 transactivator of transcription (Tat) and the resultant Tat–AIE nanoparticles could trace live cells for 10–12 passages *in vitro*.¹⁵

Fluorescent cellular tracing for even longer periods of time is desirable and useful for many biomedical applications (vide supra). In this work, we functionalized TPE with a reactive isothiocyanate (ITC) group. The obtained TPE–ITC adduct was used to label chitosan (CS), a cytocompatible biopolymer derived from shells of crabs, shrimps, lobsters, etc. (Scheme 1). The AIE attribute of TPE–ITC enabled fabrication of highly fluorescent TPE–CS bioconjugates through the attachment of a large number of AIE labels to a CS chain. The fluorescence output of the bioconjugate can be enhanced to a great extent (up to 2 orders of magnitude) by simply increasing its DL. The

Scheme 1. Synthesis of a Bioconjugate of Tetraphenylethene (TPE) and Chitosan (CS)^a



^aBy the addition reaction of the isothiocyanate (ITC) group in TPE–ITC with the amino group in CS.

highly emissive bioconjugates can enter living cells in a noninvasive manner. While the nanoparticles in our previous work were fabricated by multistep procedures,¹⁵ the TPE–CS bioconjugates in this work spontaneously cluster into microparticles inside live cells. The internalized microparticles do not leak out from the intracellular compartments and can trace the living cells for as long as 15 passages.

2. RESULTS AND DISCUSSION

Synthesis of TPE–ITC Adduct. Since our first report on the AIE behavior of TPE,¹⁶ many TPE derivatives have been prepared.¹⁰ In this work, we prepared a TPE–ITC adduct, i.e., 1-[4-(isothiocyanatomethyl)phenyl]-1,2,2-triphenylethene, by the synthetic route shown in Scheme S1 in the Supporting Information (SI).¹⁷ The product was characterized by standard spectroscopic techniques, from which satisfactory analysis data corresponding to its expected molecular structure were obtained. The product, for example, shows peaks at δ 4.63 and 48.75 in its ¹H (Figure 1a) and ¹³C (Figure S1a in the SI) NMR spectra, respectively, due to the resonance of the methylene unit between the TPE and ITC units, while the peak at $m/z = 403.1386$ in the HRMS spectrum (Figure S2, SI) perfectly matches the theoretical mass of the adduct ($m/z = 403.1395$).

TPE–ITC is AIE active, like many other TPE derivatives previously prepared in our groups.¹⁰ As seen from Figure 2a, practically no photoluminescence (PL) signals are collected from the dilute THF solution of TPE–ITC. Its phenyl rings undergo active intramolecular rotations in the THF solution, which nonradiatively annihilates its excited states and renders it nonemissive in the solution state.^{7,8} However, when a large amount of water ($f_w > 70$ vol %) is admixed with THF, the fluorogen starts to radiate. In the THF/water mixture with an f_w of 90%, its PL intensity (I) becomes $\sim 36,200$ -fold stronger than that in the THF solution (I_0). In the aqueous mixtures with high f_w values, the fluorogenic molecules aggregate. In the aggregates, intramolecular rotations of the aromatic rotors of the fluorogens are physically hindered. This restriction of the intramolecular rotations (RIR) blocks nonradiative decay channels and populates radiative transitions, thus making the aggregates highly fluorescent.^{8–10}

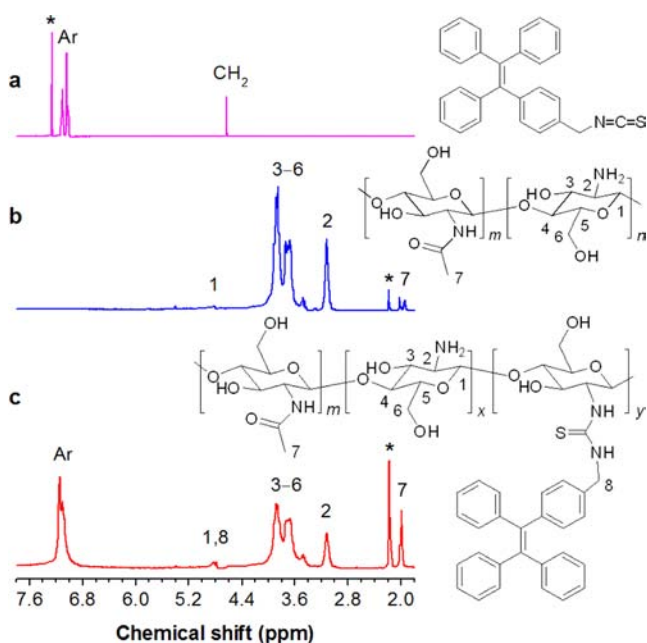


Figure 1. ^1H NMR spectra of (a) TPE-ITC, (b) CS, and (c) TPE-CS measured in (a) chloroform- d and (b, c) an acetic acid- d_4 /water- d_2 mixture at room temperature. The solvent peaks are marked with asterisks.

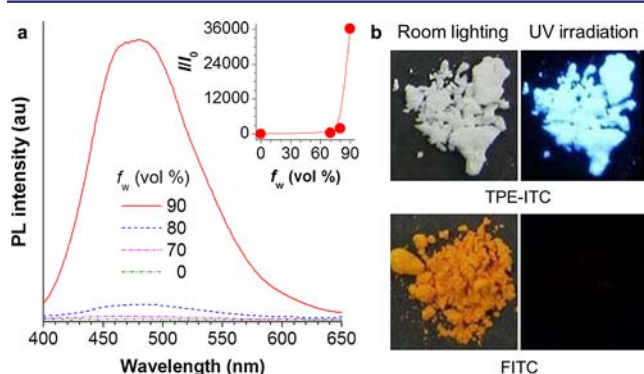


Figure 2. (a) PL spectra of TPE-ITC in THF/water mixtures with different fractions of water (f_w); $c = 50 \mu\text{M}$, $\lambda_{\text{ex}} = 338 \text{ nm}$. (Inset) Plot of the relative PL intensity (I/I_0) of TPE-ITC at 479 nm vs the composition of the THF/water mixture (f_w). $I_0 = \text{PL intensity of TPE-ITC in THF solution}$. (b) Photographs of solid powders of TPE-ITC and fluorescein isothiocyanate (FITC) taken under room lighting and UV illumination.

The solid powders of TPE-ITC are gray in appearance under normal room lighting and emit a strong greenish-blue light upon UV illumination (Figure 2b, upper panel). This is very different from the fluorescence behaviors of the conventional ACQ fluorophores. FITC, for example, is a fluorescein (F) dye functionalized by an isothiocyanate (ITC) unit that is reactive toward an amino group in a biopolymer (such as protein). It has been utilized as a fluorescent dye in an array of biological applications (e.g., flow cytometry). Though FITC is emissive in dilute solutions, its solid powders are non-fluorescent under UV excitation, as can be seen from the photograph shown in the lower panel of Figure 2b, due to the severe self-quenching effect in the dye aggregates.

Labeling CS Chains with TPE Fluorogens. CS chains were labeled by the AIE-active TPE units via the synthetic route shown in Scheme 1.¹⁸ For the purpose of comparison, the CS

chains were also labeled by fluorescein (F), an ACQ unit, by the same synthetic route (Scheme S2 in the SI). The analysis data of the resultant FCS bioconjugates are in nice agreement with those reported in the literatures,^{18,19} with the examples of NMR spectra of a TPE-CS bioconjugate shown in Figures 1 and S1 (SI). The resonance peaks of the protons of the phenyl rings of the TPE-CS bioconjugate and the carbons of its phenyl rings/olefin double bond appear at δ 7.50–6.70 and 132.1–128.8 in the ^1H and ^{13}C NMR spectra, respectively. The appearance of these new peaks confirms the successful labeling of the CS chains by the TPE units.

The efficiencies of labeling by the bioconjugation reactions were evaluated by UV, PL and NMR analyses.^{18,19} At a feed ratio ($R_f = \text{TPE/CS}$) of 1 mol %, the DL of the TPE-CS bioconjugate determined by UV analysis is 0.88 mol % (Table S1 in the SI). The DL is increased with an increase in R_f . When the R_f is increased to 20 mol %, the DL reaches 7.20 mol %. The DLs of the TPE-CS bioconjugates calculated from the NMR spectral data are in good agreement with those obtained from the UV data. The DL of the FCS bioconjugate prepared at an R_f of 1 mol % is too low to be determined by the UV and NMR analyses. Using the highly sensitive PL technique, the DL of the bioconjugate is estimated to be 0.09 mol %. Even when the R_f is increased to as high as 10 mol %, the DL of the FCS bioconjugate is still as low as 0.52 mol %.

All the DLs of the TPE-CS bioconjugates are much higher than those of their FCS congeners (Table S1, SI), indicating that TPE-ITC is much more reactive than FITC. This can be readily comprehended from the difference in their structures. In TPE-ITC, there is a methylene spacer between the phenyl ring and the ITC group. This saturated spacer shuts down the electronic interaction between the ITC and phenyl units and mitigates the steric hindrance effect of the phenyl ring, thus rendering the ITC group very reactive. In FITC, however, the ITC group is directly linked to the phenyl ring. The electronic and steric effects collectively passivate the ITC group, making it difficult to label the CS chain. Indeed, other researchers have reported the similarly low DLs in their systems of CS labeling by FITC.¹⁸

The appearances of solid powders of the TPE-CS and FCS bioconjugates are whitened and darkened, respectively, with increases in their DLs (Figure S3 in the SI). When the solid powder of the TPE-CS bioconjugate with a DL of 0.83 mol % is excited by a UV light, it emits a greenish-blue light (Figure 3a). The fluorescence of the bioconjugate is intensified with an increase in its DL: the more the TPE labels, the stronger the

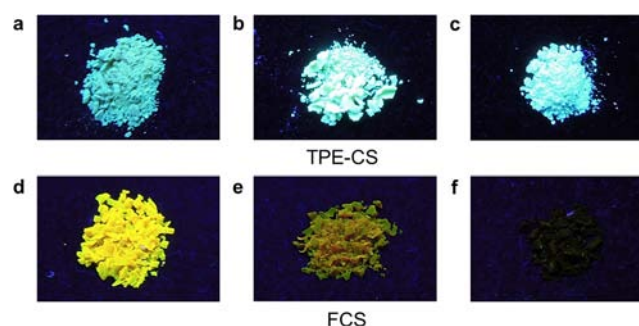


Figure 3. Fluorescent images of (a–c) TPE-CS and (d–f) FCS bioconjugates with degrees of labeling (DLs; mol %) of (a) 0.83, (b) 2.77, (c) 7.86, (d) 0.09, (e) 0.11, and (f) 0.52. The photographs were taken under UV illumination (365 nm).

light emission (cf. panels a–c). This suggests that the TPE–CS conjugates are AIE active. A diametrically opposed effect is observed in the case of the FCS bioconjugate. While the FCS conjugate with a DL of 0.09 mol % emits a bright-yellow light, the emission is drastically weakened with an increase in its DL (panels d–f). The FCS bioconjugate with a DL of 0.52 mol % becomes totally nonfluorescent, due to the ACQ effect of the fluorescein aggregates in the “heavily” labeled FCS system.

AIE Behaviors of TPE–CS Bioconjugates. The AIE effect of the TPE–CS bioconjugates suggested by the fluorescent images shown in panels a–c of Figure 3 was further studied spectroscopically. The PL spectra of the dilute solutions of TPE and CS run nearly parallel to the abscissa, verifying their nonemissive nature in the solution state.¹⁰ The TPE–CS bioconjugates are soluble in acidic media (aqueous acetic acid with pH 5 being used as the solvent in this work). However, different from those of their parent forms (TPE and CS), the dilute solutions of the TPE–CS bioconjugates are fluorescent (Figure 4a). When a TPE group is bound to a CS backbone,

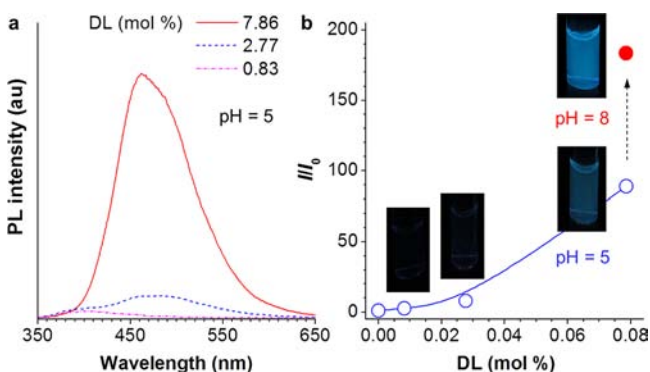


Figure 4. (a) PL spectra of TPE–CS bioconjugates with different DLs measured in 0.1 M aqueous acetic acid at [TPE–CS] = 0.1 mg/mL. (b) Plot of the relative PL intensity (I/I_0) of TPE–CS vs its DL. I_0 = PL intensity in 0.1 M acetic acid solution. Inset: Fluorescent images of the TPE–CS solutions taken at pH = 5 and pH = 8 under UV illumination.

the intramolecular rotations of its phenyl rings are not as easy as in the unbound, “free” state. This activates the RIR process, thus making the TPE–CS bioconjugate fluorescent even in the solution state.^{8–10}

The fluorescence intensity of the TPE–CS bioconjugate is increased with an increase in its DL in a nonlinear fashion (Figure 4b). The bioconjugate with a high DL of 7.86 mol % is much more fluorescent than its counterpart with a low DL of 0.83 mol %: the light emission of the former is >35-fold more intense than that of the latter. The heavy labeling of the CS chain by the hydrophobic TPE fluorogens may have decreased the miscibility of the macromolecular chain with the aqueous medium. The polymer chain may have entangled or wrapped the TPE fluorogen and strengthened the RIR process, thereby nonlinearly boosting its fluorescence.

When the pH of the aqueous medium is changed from 5 to 8, the PL intensity of the TPE–CS bioconjugate is jumped by more than 2 times, as clearly shown by the intense blue light emitted from the sample vial in Figure 4b. The dissolution of the TPE–CS bioconjugate in the acidic medium is realized by the ionization or quaternization of the amino units in the CS chain. When the acidic medium (pH 5) is changed to a basic one (pH 8), the quaternized or ionized macromolecular chain

is changed to a neutral one, which is immiscible with the aqueous medium. The polymer chains therefore contract in conformation and form aggregates that wrap the TPE labels. This prompts the RIR process and brightens the emission of the TPE–CS bioconjugate.

Live Cell Imaging. Being a biomacromolecule from the natural resources, CS is cytophilic.²⁰ The novel AIE effect of the TPE–CS bioconjugates encouraged us to utilize them as bioprobes for cellular imaging applications. HeLa cells were cultured in the aqueous buffers containing the bioconjugates at pH 6.2 using a standard cell-staining protocol. As can be seen from Figure 5, the living HeLa cells cultured in the presence of

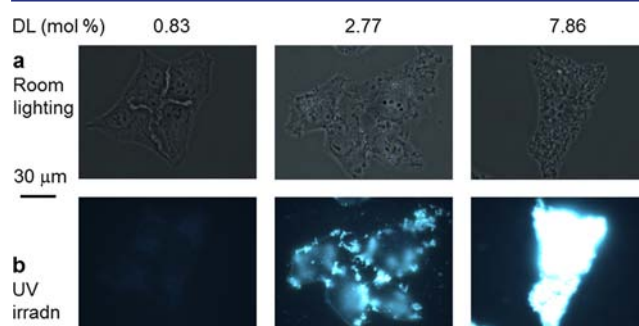


Figure 5. (a) Bright-field and (b) fluorescent images of the HeLa cells cultured in the presence of the TPE–CS bioconjugates with different DLs. [TPE–CS] = 0.1 mg/mL, pH = 6.2. Photographs taken under (a) room lighting and (b) UV irradiation.

the TPE–CS bioconjugate with a DL of 0.83 mol % emits a weak light, in accordance with its weak PL spectrum shown in Figure 4a. When the DL of the bioconjugate is increased to 2.77 mol %, the stained cells become emissive. Very bright light is emitted from the living HeLa cells stained by the bioconjugate with a DL of 7.86 mol %.

In our previous work, a commercially available dye named CellTracker Green CMFDA (or 5-chloromethylfluorescein diacetate)² was used to stain HeLa cells.²¹ The fluorescence process of the commercial dye was activated by the esterase hydrolysis with the involvement of an addition reaction of its benzyl chloride moiety to the intracellular thiol unit. No chemical reactions are involved in our cellular staining system. The light emissions of the TPE–CS bioconjugates are triggered by a rapid physical process of spontaneous aggregation of the internalized AIE fluorogen molecules inside the cellular compartments.

The intracellular imaging processes of our AIE-active TPE–CS bioconjugates were further scrutinized by the careful 3D analysis using a confocal laser scanning microscope.²² The extracellular bioconjugate molecules dissolved in the culture media (pH = 6.2) had been thoroughly washed away before the image was taken. As can be seen from the projections of the 3D image onto the x – z and y – z planes shown in Figure 6a, the PL signals are from the TPE–CS bioconjugates internalized by the HeLa cells. The bioconjugate molecules engulfed by the live cells form aggregates, as the TPE-labeled CS chains are insoluble in the cytosols at the intracellular pH (7.2–7.4; Figure S4). The intracellular aggregates emit brightly, thanks to the AIE nature of the TPE labels.

Leakage-Free Staining. Conventional fluorophores can hardly be retained inside live cells for a long period of time under physiological conditions. It is very difficult for them to survive the passage processes, during which they are easily

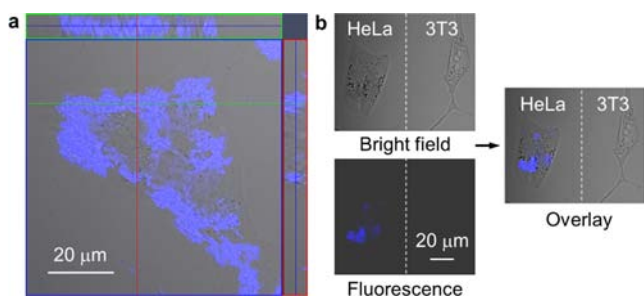


Figure 6. (a) Optical section (x - y axis) captured by confocal laser scanning microscope, with projections on x - z and y - z planes, of the HeLa cells incubated in the presence of a solution (0.1 mg/mL) of a TPE-CS bioconjugate with a DL of 7.86 mol %. (b) Bright-field, fluorescence, and overlay images of the TPE-CS-stained HeLa cells cocultured with unstained 3T3 cells.

extruded back to the growth media. To examine if the TPE-CS bioconjugates will diffuse from the intracellular compartments to the extracellular media, the HeLa cells stained by the TPE-CS bioconjugates were cocultured with unstained 3T3 cells in Petri dishes. These two types of cell lines are chosen in this study because of their distinct cell morphologies.

After overnight coculture, the aggregates of the TPE-CS bioconjugates remain inside the living HeLa cells, as verified by the intense PL signals collected from these cells (Figure 6b). On the other hand, the 3T3 cells in the same Petri dish remain nonfluorescent, revealing that the TPE-CS bioconjugates have neither escaped from the HeLa cells nor penetrated into the 3T3 cells in the coculture media. As discussed above, the conventional dyes usually function as single molecular species in the cellular imaging systems, which can be easily extruded out from the cells, unless they are bound by the covalent bonds generated by in situ chemical reactions with the intracellular reactive species such as thiol.^{2,23} The TPE-CS bioconjugates function as supramolecular aggregates, which are difficult to extrude out once they are internalized,^{14,21} which accounts for their remarkable leakage-free staining behaviors.

Long-Term Tracing. The leakage-free retention of the TPE-CS bioconjugates in the stained cells suggests that they can serve as fluorescent bioprobes for long-term cell tracing. This is indeed the case. The living cells stained by the heavily labeled CS chains emit intensely at the first passage (Figure 7).

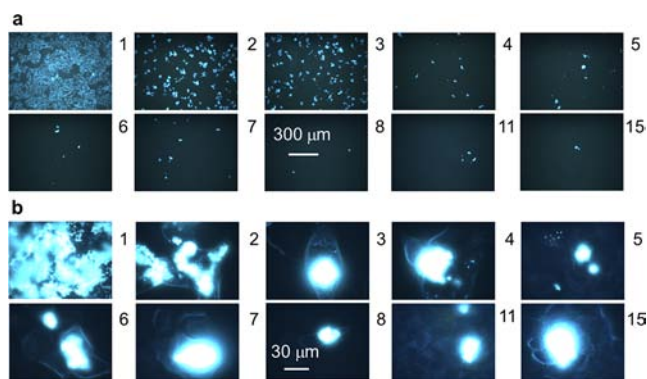


Figure 7. Fluorescent images of the HeLa cells stained by the aggregates of the TPE-CS bioconjugate with a DL of 7.86 mol % at different passages taken at magnifications of (a) $\times 100$ and (b) $\times 1000$. Numbers of passages are denoted by the Arabic numerals (1–15) on the right sides of the images.

In the case of bioimaging using small-molecule fluorophores, fluorescence of the stained cells is often drastically weakened with an increase in the number of passages. The TPE-CS bioconjugate is a big polymer and behaves differently from its small-molecule counterpart. The fluorescence intensity of the stained cells does not change much, while the relative number of the stained cells decreases rapidly with increasing number of passages. This implies that the aggregates of the TPE-CS bioconjugate are not uniformly split during the process of cell division (Figure S5, SI).

The persistence in the fluorescence signals from the stained live cells monitored in the first five days was evaluated by a confocal microscope (Figure S6, SI). The experimental data further confirm that the stained live cells can retain the high fluorescence intensities as the original ones in a long period of time. To our delight, the stained cells still fluoresce brightly even for as long as 15 passages (Figure 7b). It is worth noting that CellTracker Green CMFDA, the best-known cellular tracer, can track the living cells for no more than three passages.²⁴

In our previous study, MitoTracker Green FM (MTG) and an aminated silole, both being small molecules, were used for cell tracing studies.¹⁴ Virtually no fluorescence signals were detected in the MTG-stained cells after the first passage, owing to the low working concentration of MTG (in the low nanomolar range to avoid the nonspecific staining and inherent cytotoxicity).² The aminated silole performed better and could trace the live cells for four passages, due to its high working concentration (in the range of mM) and the slow release of its internalized nanoparticles to the fresh cell growth media.¹⁴ The cellular imaging performance of the TPE-CS bioconjugate is even better, thanks to its polymeric nature and to the big sizes of its aggregates, which makes it difficult for the internalized microparticles to escape from the cellular enclosures and to break down in the cell division processes.

In a conventional system, even if a zero rate of dye efflux is assumed, 15 times of cell divisions will lead to a 2^{15} - or 32,768-fold dilution of the dye signal, which makes the labeled cells undistinguishable. In our system, large AIE aggregates are preserved in one cell, instead of being averaged to two daughter cells in every cell division cycle. The long retention duration of the microparticles of the TPE-CS bioconjugates in a specific preloaded cell line may enable their use in a variety of unique biomedical applications as long-term cellular tracers for monitoring biological processes, pathological pathways, therapeutic effects, and so on.

3. CONCLUSIONS

In this work, we have designed and synthesized a TPE-ITC adduct with AIE characteristics. The insertion of a saturated flexible methylene spacer between the phenyl ring and the ITC group has helped alleviate the detrimental effects caused by the electronic interaction and steric hindrance. This renders TPE-ITC more reactive than FITC, a widely used fluorescent labeling reagent for bioimaging. The high reactivity of TPE-ITC has enabled more TPE labels to be attached to a CS chain. Whereas the fluorescence of the FCS bioconjugate is quickly quenched when its DL is slightly increased due to the ACQ effect commonly observed in the conventional fluorophore systems, the emission of the TPE-CS bioconjugate is boosted with an increase in its DL, thanks to the unique AIE effect of the TPE label.

Some of the TPE labels attached to the CS backbones may be wrapped by the polymer chains. After being strangled by the polymer chains, the phenyl rotors of TPE become difficult to undergo intramolecular rotations. This RIR process hampers the excited states of TPE from nonradiatively decaying. In the TPE–CS bioconjugate with a DL of 7.86 mol %, the heavily labeled CS chain becomes more hydrophobic and less miscible with the aqueous medium, which further strengthens the RIR process, thereby rendering the TPE–CS bioconjugate highly fluorescent. The bioconjugate becomes more emissive when the pH of the medium is increased (from acidic to alkaline), owing to the decrease in its solubility in the medium and the aggregate formation of its molecules at high pH.

The AIE activity and pH sensitivity of the bioconjugates have enabled them to work as fluorescent light-up bioprobes for intracellular imaging applications. When internalized, the TPE-labeled CS chains become insoluble and spontaneously form microparticles at intracellular pH. This triggers the AIE processes of the bioconjugates and makes the stained live cells highly emissive. The internalized microparticles do not leak out in the coculture system, allowing visual differentiation of one specific cell line from the other unstained cell lines. The outstanding intracellular retention of the TPE–CS bioconjugate microparticles permits the stained cells to be traced for as long as 15 passages. This makes the TPE–CS conjugates promising candidate materials for applications in biomedical areas as long-term cellular tracers which are under high demand in such important areas as cancer metastasis, neuron networking, embryo development, and stem cell differentiation.

4. EXPERIMENTAL SECTION

General Information. All the chemicals and reagents were purchased from Sigma and Aldrich and used without further purification, unless specified otherwise. THF, toluene, and dichloromethane were purified by simple distillation prior to use. 1-[4-(Azidomethyl)phenyl]-1,2,2-triphenylethylene (**6** in the SI) was prepared using previously reported procedures.¹⁷ ¹H and ¹³C NMR spectra were measured on a Bruker ARX 400 spectrometer. HRMS spectra were taken on a Finnigan TSQ 7000 triple quadrupole spectrometer operating in the MALDI-TOF mode. UV–vis absorption spectra were recorded on a Milton Ray Spectronic 3000 array spectrophotometer, and PL spectra were measured on a Perkin-Elmer LS 50B spectrofluorometer with a xenon discharge lamp excitation.

Synthesis of TPE–ITC. The azido-functionalized TPE (**6**; 0.330 g, 0.852 mmol) and triphenylphosphine (0.112 g, 0.426 mmol) were added into a two-necked flask, which was evacuated under vacuum and flushed with dry nitrogen three times. Carbon disulfide (0.55 g, 7.242 mmol) and distilled dichloromethane (50 mL) were added into the flask under stirring. The resultant reaction mixture was refluxed overnight, followed by the removal of the solvent under a reduced pressure. The crude product was precipitated with cold ether (250 mL), and the precipitate was filtered and washed with cold ether (30 mL) three times. The product was dried under vacuum to give a white solid in 85.2% yield. ¹H NMR (400 MHz, CDCl₃) δ (ppm): 7.00–7.13 (m, 19H), 4.63 (s, 2H). HRMS (MALDI-TOF) *m/e*: 403.1386 ([M]⁺, calcd: 403.1395).

Degradation of CS. Six (6) grams of CS with a viscosity-average molecular weight (M_{η}) of 1.16×10^6 was added into a mixture of distilled water (190 mL) and acetic acid (4 mL), which was stirred for 1 h at room temperature and then heated

to 65 °C. Hydrogen peroxide (6 mL) was added into the CS solution, and the mixture was stirred at 65 °C for 6 h. The thus-treated CS was precipitated with a 10% sodium hydroxide solution, filtered, and washed with distilled water until the pH became neutral. The collected precipitate was lyophilized at –50 °C for three days. The deacetylation degree of CS was 93.64%, as determined by conductometric titration using a conductivity meter (DDS-307).²⁵ The M_{η} value of the CS was decreased by the degradation reaction to 5.60×10^4 , as estimated by the molecular weight measurement with an Ubbelohde viscometer at 25 ± 0.5 °C using a mixture of 0.1 M acetic acid and 0.2 M sodium acetate as the solvent.

Labeling of CS by TPE–ITC. The degraded CS (0.1 g, 0.61 mmol) was added into a two-necked flask, evacuated under vacuum and flushed with dry nitrogen three times. DMSO (10 mL) was added into the flask, and the mixture was stirred at 60 °C for 24 h. A specific amount of TPE–ITC (with R_f in the range of 1–20 mol %) was added into the flask, and the resultant mixture was stirred for 24 h. The product was washed with distilled water five times and acetone three times and then was dissolved in an aqueous mixture of acetic acid with an equal volume of acetone. The solution was precipitated with a 10% sodium hydroxide solution, filtered, and washed with distilled water until the pH became neutral. The product was dried under vacuum at 60 °C. The labeling experiments of CS by FITC ($R_f = 1$ –10 mol %) were conducted as a control by employing the published experimental procedures.¹⁸ The labeling efficiencies or DLs of the TPE–CS and FCS bioconjugates were determined by UV, PL, and NMR analyses,^{18,26} and the results are summarized in Table S1 in the SI.

Cellular Imaging. HeLa cells were grown overnight on a cover slide in a 35-mm Petri dish. The living cells were stained with a solution of a TPE–CS bioconjugate (100 μ g/mL) and were further incubated for another 4 h. After careful washing, fluorescence images of the stained cells were taken on a fluorescence microscope (Olympus BX41) with a long-pass emission filter using the following parameters: excitation wavelength = 330–380 nm and dichroic mirror = 400 nm.

Coculture of HeLa and 3T3 Cells. HeLa cells were stained with a TPE–CS solution (100 μ g/mL) for 4 h. After washing five times with PBS, the stained HeLa cells and the unstained 3T3 cells were detached from their respective culture dishes by treating them with trypsin–EDTA solution. The stained HeLa cells (1.5×10^3) and the unstained 3T3 cells (2.5×10^3) were resuspended with 2 mL of DMEM and then transferred to a new 25-mm Petri dish. After incubating at 37 °C for 12 h, phase contrast and fluorescence images of the cocultured cells were taken from the same spot using a Zeiss laser scanning confocal microscope (LSM7 DUO; excitation: 405 nm, filter: 449–520 nm).

Long-Term Cell Tracing. Living HeLa cells (3×10^4) were cultured overnight and then stained in a Petri dish at 50% confluence with a TPE–CS solution (100 μ g/mL). After an image was taken at the end of 24 h of incubation (referred to as the end of the first passage), 25% of the cells in the completely filled Petri dish were transferred to a new dish with fresh growth medium. Another image was taken after 24 h in the then half-filled Petri dish, i.e., the end of the second passage. The living cells were further incubated for another 24 h to the end of the third passage. This process was iterated to proceed to the 15th passage.

■ ASSOCIATED CONTENT

■ Supporting Information

Schemes depicting the synthetic routes to TPE-ITC and FCS; a table listing the DLs of the TPE-CS and FCS bioconjugates; and figures showing the ^{13}C NMR spectra of TPE-ITC, CS and TPE-CS, the HRMS spectrum of TPE-ITC, the photographs of the TPE-CS and FCS bioconjugates with different DLs, dynamic uptake process of TPE-CS by HeLa cell, dynamic distribution of TPE-CS during the cell division, intensities of the fluorescent signals from the stained cells, and cytotoxicity data. This material is available free of charge via the Internet at <http://pubs.acs.org>.

■ AUTHOR INFORMATION

Corresponding Author

tangbenz@ust.hk

Author Contributions

[§]Z.W. and S.C. contributed equally to this work.

Notes

The authors declare no competing financial interest.

■ ACKNOWLEDGMENTS

The work reported in this paper was partly supported by National Basic Research Program of the Ministry of Science and Technology of China (973 Program; 2013CB834701), the Research Grants Council of Hong Kong (HKUST2/CRF/10 and N_HKUST620/11), the University Grants Committee of Hong Kong (AoE/P-03/08), and the Guangdong Innovative Research Team Program of China (201101C0105067115).

■ REFERENCES

- (1) For selected examples of reviews, see: (a) Woolf, N. J. *Prog. Neurobiol.* **1998**, *55*, 59–77. (b) Nemoto, T. *Mol. Cells* **2008**, *26*, 113–120. (c) Mattoussi, H.; Palui, G.; Na, H. B. *Adv. Drug Delivery Rev.* **2012**, *64*, 138–166. (d) Taylor, A.; Wilson, K. M.; Murray, P.; Fernig, D. G.; Levy, R. *Chem. Soc. Rev.* **2012**, *41*, 2707–2717. (e) Dreaden, E. C.; Alkilany, A. M.; Huang, X.; Murphy, C. J.; El-Sayed, M. A. *Chem. Soc. Rev.* **2012**, *41*, 2740–2779.
- (2) (a) Johnson, I., Spence, M. T. Z., Eds. *The Molecular Probes Handbook: A Guide to Fluorescent Probes and Labeling Technologies*, 11th ed.; Life Technologies Corp.: New York, 2010. (b) Herold, K. E., Rasooly, A., Eds. *Biosensors and Molecular Technologies for Cancer Diagnostics*; Taylor & Francis: Oxford, 2012. (c) Thompson, R. B., Ed. *Fluorescence Sensors and Biosensors*; CRC Press: Boca Raton, FL, 2005.
- (3) For reviews, see: (a) Yao, S.; Belfield, K. D. *Eur. J. Org. Chem.* **2012**, *17*, 3199–3217. (b) Kim, W. H.; Lee, J.; Jung, D.-W.; Williams, D. R. *Sensors* **2012**, *12*, 5005–5027. (c) Coto-Garcia, A. M.; Sotelo-Gonzalez, E.; Fernandez-Arguelles, M. T.; Pereira, R.; Costa-Fernandez, J. M.; Sanz-Medel, A. *Anal. Bioanal. Chem.* **2011**, *399*, 29–42. (d) Tanury, P.; Malhotra, A.; Byrne, L. M.; Santra, S. *Adv. Drug Delivery Rev.* **2010**, *62*, 424–437. (e) Escobedo, J.; Rusin, O.; Lim, S.; Strongin, R. M. *Curr. Opin. Chem. Biol.* **2010**, *14*, 64–70. (f) Meech, S. R. *Chem. Soc. Rev.* **2009**, *38*, 2922–2934. (g) Terai, T.; Nagano, T. *Curr. Opin. Chem. Biol.* **2008**, *12*, 515–521.
- (4) (a) Yang, P.-Y.; Wang, M.; Li, L.; Wu, H.; He, C. Y.; Yao, S. Q. *Chem.—Eur. J.* **2012**, *18*, 6528–6541. (b) Wang, G.; Geng, J.; Zhang, X.; Cai, L.; Ding, D.; Li, K.; Wang, L.; Lai, Y.-H.; Liu, B. *Polym. Chem.* **2012**, *3*, 2464–2470. (c) Gasser, G.; Pinto, A.; Neumann, S.; Sosniak, A. M.; Seitz, M.; Merz, K.; Heumann, R.; Metzler-Nolte, N. *Dalton Trans.* **2012**, *41*, 2304–2313. (d) Singh, S.; Aggarwal, A.; Thompson, S.; Tome, J. P. C.; Zhu, X.; Samaroo, D.; Vinodu, M.; Gao, R.; Drain, C. M. *Bioconjugate Chem.* **2010**, *21*, 2136–2146.
- (5) (a) Qin, A.; Lam, J. W. Y.; Tang, B. Z. *Prog. Polym. Sci.* **2012**, *37*, 182–209. (b) Qin, A.; Lam, J. W. Y.; Tang, B. Z. *Chem. Soc. Rev.* **2010**,

39, 2522–2544. (c) Qin, A.; Lam, J. W. Y.; Tang, B. Z. *Macromolecules* **2010**, *43*, 8693–8702.

(6) (a) Nadeau, J. *Introduction to Experimental Biophysics*; CRC Press: Boca Raton, FL, 2011. (b) Orellana, G., Moreno-Bondi, M. C., Eds. *Frontiers in Chemical Sensors: Novel Principles and Techniques*; Springer: Berlin, 2010. (c) Birks, J. B. *Photophysics of Aromatic Molecules*; Wiley: London, 1970.

(7) Luo, J.; Xie, Z.; Lam, J. W. Y.; Cheng, L.; Chen, H.; Qiu, C.; Kwok, H. S.; Zhan, X.; Liu, Y. Q.; Zhu, D. B.; Tang, B. Z. *Chem. Commun.* **2001**, 1740–1741.

(8) (a) Hong, Y.; Lam, J. W. Y.; Tang, B. Z. *Chem. Soc. Rev.* **2011**, *40*, 5361–5388. (b) Wang, M.; Zhang, G.; Zhang, D.; Zhu, D.; Tang, B. Z. *J. Mater. Chem.* **2010**, *20*, 1858–1867. (c) Hong, Y.; Lam, J. W. Y.; Tang, B. Z. *Chem. Commun.* **2009**, 4332–4353. (d) Liu, J.; Lam, J. W. Y.; Tang, B. Z. *Chem. Rev.* **2009**, *109*, 5799–5867.

(9) For a review, see: Liu, J.; Lam, J. W. Y.; Tang, B. Z. *J. Inorg. Organomet. Polym. Mater.* **2009**, *19*, 249–285.

(10) (a) Zhao, Z.; Lam, J. W. Y.; Tang, B. Z. *Curr. Org. Chem.* **2010**, *14*, 2109–2131. (b) Zhao, Z.; Lam, J. W. Y.; Tang, B. Z. *J. Mater. Chem.* **2012**, *22*, 23726–23740.

(11) For reviews, see: (a) Chi, Z.; Zhang, X.; Xu, B.; Zhou, X.; Ma, C.; Zhang, Y.; Liu, S.; Xu, J. *Chem. Soc. Rev.* **2012**, *41*, 3878–3896. (b) Salinas, Y.; Martinez-Manez, R.; Marcos, M. D.; Sancenon, F.; Costero, A. M.; Parra, M.; Gil, S. *Chem. Soc. Rev.* **2012**, *41*, 1261–1296. (c) Tanaka, K.; Chujo, Y. *Macromol. Rapid Commun.* **2012**, *33*, 1235–1255. (d) Anthony, S. P. *ChemPlusChem* **2012**, *77*, 518–531. (e) Akiyama, S. *J. Synth. Org. Chem. Jpn.* **2012**, *70*, 465–472. (f) Hatano, K.; Matsuoka, K.; Terunuma, D. *Trends Glycosci. Glycotechnol.* **2012**, *24*, 78–94. (g) Yang, G.; Li, S.; Wang, S.; Li, Y. C. R. *Chim.* **2011**, *14*, 789–798. (h) Yuan, C.; Xin, Q.; Liu, H.; Wang, L.; Jiang, M.; Tao, X. *Sci. China, Ser. B* **2011**, *54*, 587–595. (i) Strassert, C. A.; Mauro, M.; De Cola, L. *Adv. Inorg. Chem.* **2011**, *63*, 47–103. (j) Corey, J. Y. *Adv. Organomet. Chem.* **2011**, *59*, 1–180. (k) Kim, H. N.; Guo, Z.; Zhu, W.; Yoon, J.; Tian, H. *Chem. Soc. Rev.* **2011**, *40*, 79–93. (l) Wu, J.; Liu, W.; Ge, J.; Zhang, H.; Wang, P. *Chem. Soc. Rev.* **2011**, *40*, 3483–3495. (m) Accetta, A.; Corradini, R.; Marchelli, R. *Top. Curr. Chem.* **2011**, *300*, 175–216. (n) Shimizu, M.; Miyahara, T. *Chem.—Asian J.* **2010**, *5*, 1516–1531. (o) Chan, C. P.-Y. *Bioanalysis* **2009**, *1*, 115–133. (p) Zhao, Y. S.; Fu, H.; Peng, A.; Ma, Y.; Xiao, D.; Yao, J. *Adv. Mater.* **2008**, *20*, 2859–2876. (q) Yang, B.; Ma, Y.-G.; Shen, J.-C. *Chem. J. Chin. Univ.* **2008**, *29*, 2643–2658. (r) Chen, J.; Cao, Y. *Macromol. Rapid Commun.* **2007**, *28*, 1714–1742. (s) Itami, K.; Ohashi, Y.; Yoshida, J. *J. Org. Chem.* **2005**, *70*, 2778–2792.

(12) (a) Shustova, N. B.; Ong, T.-C.; Cozzolino, A. F.; Michaelis, V. K.; Griffin, R. G.; Dincă, M. *J. Am. Chem. Soc.* **2012**, *134*, 15061–15070. (b) Tian, D.; Jiang, J.; Hu, H.; Zhang, J.; Cui, C. *J. Am. Chem. Soc.* **2012**, *134*, 14666–14669. (c) Xu, Y.; Chen, L.; Guo, Z.; Nagai, A.; Jiang, D. *J. Am. Chem. Soc.* **2011**, *133*, 17622–17625. (d) Ren, Y.; Kan, W. H.; Henderson, M. A.; Bomben, P. G.; Berlinguette, C. P.; Thangadurai, V.; Baumgartner, T. *J. Am. Chem. Soc.* **2011**, *133*, 17014–17026. (e) Perez, A.; Luis Serrano, J.; Sierra, T.; Ballesteros, A.; de Saa, D.; Barluenga, J. *J. Am. Chem. Soc.* **2011**, *133*, 8110–8113. (f) Procopio, E. Q.; Mauro, M.; Panigati, M.; Donghi, D.; Mercandelli, P.; Sironi, A.; D'Alfonso, G.; De Cola, L. *J. Am. Chem. Soc.* **2010**, *132*, 14397–14399. (g) Dong, J.; Solntsev, K. M.; Tolbert, L. M. *J. Am. Chem. Soc.* **2009**, *131*, 662–670. (h) Peng, Q.; Yi, Y.; Shuai, Z.; Shao, J. *J. Am. Chem. Soc.* **2007**, *129*, 9333–9339. (i) Yu, G.; Yin, S.; Liu, Y.; Chen, J.; Xu, X.; Sun, X.; Ma, D.; Zhan, X.; Peng, Q.; Shuai, Z.; Tang, B. Z.; Zhu, D.; Fang, W.; Luo, Y. *J. Am. Chem. Soc.* **2005**, *127*, 6335–6346. (j) Luo, Z.; Yuan, X.; Yu, Y.; Zhang, Q.; Leong, D. T.; Lee, J. Y.; Xie, J. *J. Am. Chem. Soc.* **2012**, *134*, 16662–16670.

(13) (a) Wee, K.-R.; Han, W.-S.; Cho, D. W.; Kwon, S.; Pac, C.; Kang, S. O. *Angew. Chem., Int. Ed.* **2012**, *51*, 2677–2680. (b) Li, C.; Wu, T.; Hong, C.; Zhang, G.; Liu, S. *Angew. Chem., Int. Ed.* **2012**, *51*, 455–459. (c) Jin, X.-H.; Wang, J.; Sun, J.-K.; Zhang, H.-X.; Zhang, J. *Angew. Chem., Int. Ed.* **2011**, *50*, 1149–1153. (d) Feng, J.; Tian, K.; Hu, D.; Wang, S.; Li, S.; Zeng, Y.; Li, Y.; Yang, G. *Angew. Chem., Int. Ed.* **2011**, *50*, 8072–8076. (e) Zhang, Z.; Xu, B.; Su, J.; Shen, L.; Xie,

- Y.; Tian, H. *Angew. Chem., Int. Ed.* **2011**, *50*, 11654–11657.
- (f) Shimizu, M.; Takeda, Y.; Higashi, M.; Hiyama, T. *Angew. Chem., Int. Ed.* **2009**, *48*, 3653–3656. (g) Mutai, T.; Tomoda, H.; Ohkawa, T.; Yabe, Y.; Araki, K. *Angew. Chem., Int. Ed.* **2008**, *47*, 9522–9524.
- (h) Wu, Y.-T.; Kuo, M.-Y.; Chang, Y.-T.; Shin, C.-C.; Wu, T.-C.; Tai, C.-C.; Cheng, T.-H.; Liu, W.-S. *Angew. Chem., Int. Ed.* **2008**, *47*, 9891–9894. (i) Bhongale, C. J.; Hsu, C. S. *Angew. Chem., Int. Ed.* **2006**, *45*, 1404–1408.
- (14) Yu, Y.; Feng, C.; Hong, Y.; Liu, J.; Chen, S.; Ng, K. M.; Luo, K. Q.; Tang, B. Z. *Adv. Mater.* **2011**, *23*, 3298–3302.
- (15) Li, K.; Qin, W.; Ding, D.; Geng, J.; Liu, J.; Zhang, X.; Liu, H.; Liu, B.; Tang, B. Z. *Sci. Rep.* **2013**, *3*, 1150.
- (16) Dong, Y. Q.; Lam, J. W. Y.; Qin, A.; Sun, J. X.; Liu, J.; Li, Z.; Zhang, S.; Sun, J. Z.; Kwok, H. S.; Tang, B. Z. *Appl. Phys. Lett.* **2007**, *91*, 011111-1–011111-3.
- (17) (a) Banerjee, M.; Emond, S. J.; Lindeman, S. V.; Rathore, R. J. *Org. Chem.* **2007**, *72*, 8054–8061. (b) Tang, L.; Jin, J. K.; Qin, A. J.; Yuan, W. Z.; Mao, Y.; Mei, J.; Sun, J. Z.; Tang, B. Z. *Chem. Commun.* **2009**, 4974–4976.
- (18) (a) Huang, M.; Ma, Z. S.; Khor, E.; Lim, L. Y. *Pharm. Res.* **2002**, *19*, 1488–1494. (b) Jia, X. Y.; Chen, X.; Xu, Y. L.; Han, X. Y.; Xu, Z. R. *Carbohydr. Polym.* **2009**, *78*, 323–329.
- (19) Jiang, G. B.; Quan, D. O.; Liao, K. R.; Wang, H. H. *Mol. Pharmaceutics* **2006**, *3*, 152–160.
- (20) Huang, M.; Khor, E.; Lim, L. Y. *Pharm. Res.* **2004**, *21*, 344–353.
- (21) Yu, Y.; Hong, Y.; Feng, C.; Liu, J.; Lam, J. W. Y.; Faisal, M.; Ng, K. M.; Luo, K. Q.; Tang, B. Z. *Sci. China, Ser. B* **2009**, *52*, 15–19.
- (22) (a) Wang, J.; Mei, J.; Hu, R.; Sun, J. Z.; Qin, A.; Tang, B. Z. *J. Am. Chem. Soc.* **2012**, *134*, 9956–9966. (b) Shi, H.; Kwok, R. T. K.; Liu, J.; Xing, B.; Tang, B. Z.; Liu, B. *J. Am. Chem. Soc.* **2012**, *134*, 17972–17981.
- (23) Liu, Y.; Yu, Y.; Lam, J. W. Y.; Hong, Y.; Faisal, M.; Yuan, W. Z.; Tang, B. Z. *Chem.—Eur. J.* **2010**, *16*, 8433–8438.
- (24) Christian, W.; Jonhson, T. S.; Gill, T. J. *J. Biomed. Sci. Eng.* **2008**, *1*, 163–169.
- (25) Raymond, L.; Morin, F. G.; Marchessault, R. H. *Carbohydr. Res.* **1993**, *246*, 331–336.
- (26) Kolb, H. C.; Finn, M. G.; Sharpless, K. B. *Angew. Chem., Int. Ed.* **2001**, *40*, 2004–2021.